

Design of the Collective Thomson Scattering System on HL-3 tokamak

Weichu Deng¹, Zhongbing Shi^{1*}, Peiwan Shi¹, Feng Zhang¹, Xin Yu¹, Zengchen Yang¹, Min Jiang¹, Yu Zhou¹, Yuqi Shen¹, Kexi Han¹, Liwen Hu¹ and Wulyu Zhong¹

¹Southwestern Institute of Physics, 610041 Chengdu, China

Abstract. A collective Thomson scattering (CTS) diagnostic system is being developed to measure fast-ion velocity distribution on HL-3 tokamak. A 140 GHz gyrotron belonging to electron cyclotron resonance heating (ECRH) system would be used to generate probe beam. The scattering spectra among HL-3 parameter ranges are calculated to assess diagnostic feasibility. Scattering signals will be detected by a heterodyne system, which is proposed to optimize diagnostic performance.

1 Introduction

Collective Thomson scattering (CTS) diagnostic is a powerful diagnostic to measure the velocity distribution of energetic ions which have direct influence on plasma confinement and fusion yield [1-3]. The first successful measurement of ion temperature by CTS was on TCA tokamak based on a D₂O laser, while its feasibility to measure fast-ion velocity distribution was verified on JET [4]. The re-distribution of fast ions during sawtooth crashes was found on TEXTOR [5] and ASDEX Upgrade [6] by CTS diagnostics. There are also CTS systems measuring fast-ion velocity on LHD [7] and W7-X [8], and these systems all utilize gyrotrons as source of probe beam, partly because that the frequency range of gyrotrons allows a looser scattering angle range under coherent condition.

Electromagnetic waves are actually scattered off electrons in plasma, due to the much larger specific charge of electrons. When an ion moves in plasma, electrons form Debye shielding around it and move with the ion. Therefore, ion motions generate electron density fluctuations which could be detected. The CTS spectra contain the information of fast-ion velocity, while its shape and radiation power also depend on geometrical and experimental conditions. It is important to optimize the system design, for better resolution and signal level. A 105 GHz CTS diagnostic has been developed on HL-2A. Experimental spectra including fast-ion information agree with calculation in general, though signals are partly saturated because of insufficient suppression to stray radiation [9,10]. A CTS diagnostic is under development on HL-3, in order to support study of fast-ion behaviors. The system parameters need to be designed to match HL-3 operating conditions, such as the magnetic field and the fast-ion energy.

2 Frequency and geometry

There are gyrotrons with 3 frequencies in HL-3 electron cyclotron resonance heating (ECRH) system, 68, 105 and 140 GHz, respectively. The injection power is no less than 0.5 MW for all frequencies. The frequency for CTS probe beam should propagate to scattering position through plasma without interacting with plasma waves.

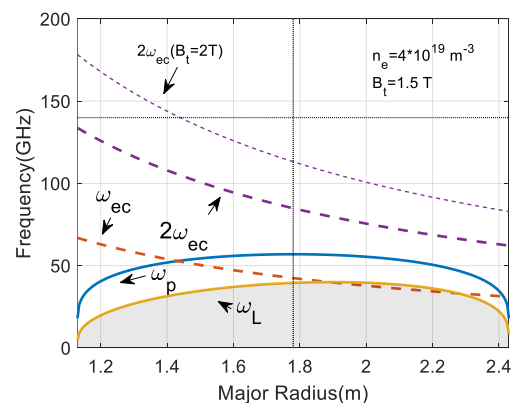


Fig. 1. Plasma frequency (ω_p), left-hand cut-off frequency (ω_L), electron cyclotron fundamental and second harmonic frequencies (ω_{ec} and $2\omega_{ec}$) against device radius. The positions of magnetic axis and 140 GHz are indicated by dotted straight line.

Some frequencies of plasma waves are shown in Fig. 1, and the shadow areas indicate where CTS probe wave or scattering wave would be bothered. Waves with frequency under left-hand cut-off frequency cannot propagate even for X mode, and O-mode waves cannot propagate under plasma frequency in plasma. Meanwhile, for probe waves in ranges of electron cyclotron fundamental and second harmonic frequencies, the X-mode probe beam would be absorbed

* Corresponding author: shizb@swip.ac.cn

and heat electrons, so it cannot be used for CTS diagnostics. The electron cyclotron emission (ECE) noise from plasma would also be received by CTS antennas and mixed with scattering signals, and an accepted solution to deduct background noises is gyrotron power modulation. Via signals during gyrotron power on subtracting signals during gyrotron power off, ECE contamination is eliminated. Therefore, O-mode probe beam in electron cyclotron fundamental and second harmonic frequencies is acceptable in CTS experiments. The CTS system on ITER [11] would use 60 GHz X-mode probe beams, as it is between left-hand cut-off frequency and upper hybrid frequency. However, the frequency gap between these two areas is not big enough on typical HL-3 operation parameters, unless in a low density and a high magnetic field. Finally we choose 140 GHz as the probe frequency of CTS diagnostic for the largest operation range, and the probe beam would be injected in O-mode. Power absorption of probe wave could still exist even if in O-mode, and it should be avoided before scattering. The position of scattering volume won't lie beyond range ρ [-0.5, 0.5], so the magnetic field under 2 T is acceptable for CTS experiments. Gyrotron power modulation will be adopted to deduct background noises.

The injection and receiving antennas are matched reflecting mirrors located in an upper port and a lower port of the adjacent section respectively. The scattering sketch is shown in Fig. 2. The injection angle of probe beam would be steerable both poloidally and toroidally, with the ranges of at least $\pm 10^\circ$. The resolved angle ϕ between the fluctuation wave and the magnetic field ranges from $90^\circ \pm 10^\circ$, while the scattering angle θ between probe wave and scattering wave ranges from $100^\circ \pm 20^\circ$.

3 Simulated spectra

The criterion of collective scattering is the Salpeter parameter [12]

$$\alpha = I/|\mathbf{k}| \lambda_D > 1 \quad (1)$$

Here, $\mathbf{k} = \mathbf{k}^s - \mathbf{k}^i$ represents the fluctuation vector defined by the scattering vector \mathbf{k}^s and the incident vector \mathbf{k}^i , and λ_D is the Debye length. With the largest scattering angle $\theta = 120^\circ$, $\alpha > 1$ would be satisfied in nearly all cases, unless $T_e/n_e > 7$ (keV/10¹⁹ m⁻³). The modeling for scattering spectrum calculation is in this study based on an electrostatic model [13] which is able to characterize the electron feature and ion feature in CTS spectra. The scattering power received can be approximated as

$$\partial P^s / \partial \omega = P^i O_b (\lambda^i)^2 r_e^2 n_e \Gamma S(\mathbf{k}, \omega) / 2\pi \quad (2)$$

where P^i is the probe power, O_b is the beam overlap, λ^i is the wavelength of the incident wave, r_e is the classical radius of electrons, n_e is the electron density, Γ is the dielectric form factor, and $S(\mathbf{k}, \omega)$ is the spectral density function of electron density fluctuations. The shape of CTS spectra depends on mainly

$$S(\mathbf{k}, \omega) = S_e(\mathbf{k}, \omega) + S_i(\mathbf{k}, \omega) + S_{fast}(\mathbf{k}, \omega) \quad (3)$$

which could be divided into three parts from bulk electrons $S_e(\mathbf{k}, \omega)$, bulk deuterium ions $S_i(\mathbf{k}, \omega)$, and fast deuterium ions $S_{fast}(\mathbf{k}, \omega)$, respectively. Fig. 3 presents the calculated spectra in the plasma center with a

magnetic field of 1.5 T, where fast ions are mainly from NBI beam ions with an energy of 100 keV. The resolved angle is set at 80° for fast-ion measurements because ion Bernstein waves would modulate the spectra when $\phi \approx 90^\circ$. Bulk ions dominate scattering spectra in 140-141 GHz, while fast-ion features are significant during 141.4-141.9 GHz, as shown in Fig 3 (a).

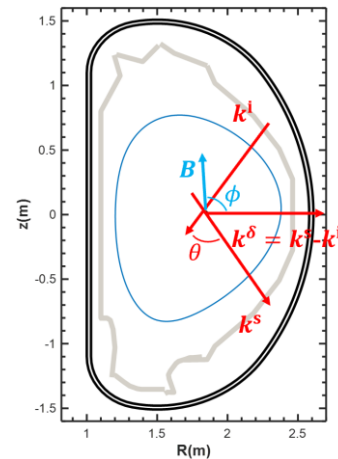


Fig. 2. The scattering sketch in plasma poloidal section. \mathbf{k}^δ , \mathbf{k}^s , \mathbf{k}^i are wave vectors of fluctuation wave, inject wave and scattering wave, indicated by red arrows. ϕ is the resolved angle and θ is the scattering angle.

Some cases with slightly different parameters are presented to qualitative their effects on spectra, ignoring the small variation in the Salpeter parameter. The difference between Fig.3 (a) and 3(c) shows that the density affects visibly signal power rather than broadening, which is obvious according to formula (2). The enhancement of ion and electron temperatures generates a large broadening on the bulk-plasma dominant range and much less effect on the fast-ion dominant range, as indicated between Fig. 3(a) and 3 (b). Electromagnetic waves scattered off charged particles with a velocity would be shifted in frequencies compared with incident waves, and the form of relation is similar to $\nu \propto \omega/|\mathbf{k}|$. A higher electron temperature means a bigger average velocity of thermal electrons which causes a bigger frequency shift, and an ion with bigger velocity drive the electron shielding to move faster. The CTS spectra broaden globally when the scattering angle increases and the calculated fast-ion dominant range is 141.5-142.1 GHz, as shown in Fig. 3(d). The value of fluctuation vector $|\mathbf{k}| \approx 2|\mathbf{k}^i| \sin(\theta/2)$, and increases with the scattering angle θ . Therefore, the same temperature corresponds to a larger broadening for a bigger scattering angle.

4 Receiver

The design of CTS receiver is similar to an ECE diagnostic system [14]. Heterodyne frequency mixing is required to distinguish the low-frequency and high-frequency parts. The receiver is a heterodyne radiometer including radio frequency (RF) part and intermediate frequency (IF) part. The RF part contains notch filters, a band-pass filter, an isolator, a LO and a mixer. Notch filters provide suppression above 80 dB around 140

GHz, to prevent damage and saturation from stray radiation. The band-pass filter with pass band 135-145 GHz filters electron cyclotron radiation, and the isolator suppresses superior modes like stand-wave. A W-band mixer and a local oscillator of 136 GHz down-convert the signals. The IF part includes a broad low-noise-amplifier (LNA), 16 filters, 16 logarithmic detectors and data acquisition. The IF frequency range is 137.5-139.5 GHz and 140.5-142.5 GHz. Each of 16 filters has a

bandwidth 100 MHz, and the interval of their central frequency is 250 MHz. As shown in Fig.3, the signal power is low in whole spectra, and the fast-ion part is smaller than around 1 eV, logarithmic detectors are essential to discern the fast-ion scattering signals. Furthermore, a transmission line with low power-loss is necessary, and over-mode corrugated waveguides will be utilized.

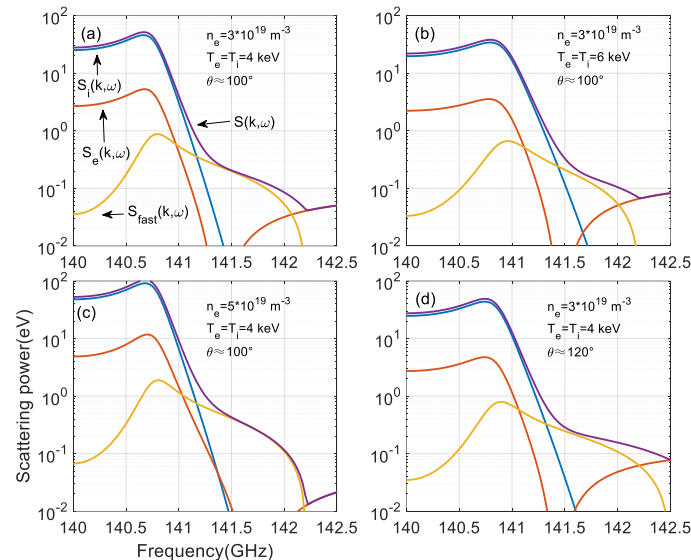


Fig. 3. Calculated CTS scattering power against the frequency on HL-3. $n_{fast}/n_e \approx 0.5\%$. Bulk ions and fast ions are both deuterium. Fast ions are slow-down NBI beam ions.

5 Summary

The design of CTS diagnostic is presented for fast-ion measurements on HL-3. The 140 GHz gyrotron is available to generate probe beam, and ECE noise could be subtracted by gyrotron modulation. Scattering spectra in different cases are calculated, and possible fast-ion dominant range is ± 1 -2.5 GHz. A heterodyne receiver is designed based on calculation.

Acknowledgments

This work is supported by National Natural Science Foundation of China (Grant No. 12175055) and the National Key R & D Program of China (Grant No. 2022YFE03040003). This work has been also partly supported by Sichuan Science and Technology Program (Grant No. 2023ZYD0014) and innovation Program of Southwestern Institute of Physics (Grants No. 202301XWCX001).

References

1. P.W. Shi, W. Chen and X.R. Duan, Energetic particle physics on the HL-2A tokamak: a review, Chinese Phys. Lett. 38 035202 (2021). <https://doi.org/10.1088/0256-307x/38/3/035202>

2. W. Chen et al., Experimental observation of multi-scale interactions among kink/tearing modes and high-frequency fluctuations in the HL-2A core NBI plasmas, Nucl. Fusion 57 114003 (2017). <https://doi.org/10.1088/1741-4326/aa7eee>
3. Z. Shi et al., Study of energetic particle physics with advanced ECEI system on the HL-2A tokamak, EPJ Web Conf. 147 01003 (2017). <https://doi.org/10.1051/epjconf/201714701003>
4. H. Bindslev, J.A. Hoekzema, J. Egedal, J.A. Fessey, T.P. Hughes and J.S. Machuzak, Fast-ion velocity distributions in JET measured by collective Thomson scattering, Phys. Rev. Lett. 83 3206 (1999). <https://doi.org/10.1103/physrevlett.83.3206>
5. S.K. Nielsen, M. Salewski, H. Bindslev et al, Dynamics of fast ions during sawtooth oscillations in the TEXTOR tokamak measured by collective Thomson scattering. Nucl. Fusion 51, 063014 (2011). <https://doi.org/10.1088/0029-5515/51/6/063014>
6. J. Rasmussen, S.K. Nielsen, M. Stejner et al, Collective Thomson scattering measurements of fast-ion transport due to sawtooth crashes in ASDEX Upgrade. Nucl. Fusion 56 112014 (2016). <https://doi.org/10.1088/0029-5515/56/11/112014>
7. S. Kubo, M. Nishiura, K. Tanaka et al, Scattering volume in the collective Thomson scattering measurement using high power gyrotron in the LHD. JINST 11 C06005 (2016). <https://doi.org/10.1088/1748-0221/11/06/C06005>

8. D. Moseev, M. Stejner, T. Stange, I. Abramovic et al, Collective Thomson scattering diagnostic at Wendelstein 7-X. Rev. Sci. Instrum. 90, 013503 (2019). <https://doi.org/10.1063/1.5050193>
9. W. C. Deng, Z. Shi, P. Shi, Z. Yang et al, Development of a 105GHz fast ion collective Thomson scattering diagnostic on HL-2A tokamak J. Instrum. 17, C02006 (2022). <https://doi.org/10.1088/1748-0221/17/02/C02006>
10. W. C. Deng, Z. Shi, P. Shi, Z. Yang et al, Preliminary results of the 105 GHz collective Thomson scattering system on HL-2A. Rev Sci Instrum 94, 094701 (2023). <https://doi.org/10.1063/5.0150123>
11. E. Tsakadze, H. Bindslev, S. B Korsholm et al, Fast Ion Collective Thomson Scattering Diagnostic for ITER: Design Elements. Sci. Technol. 53, 69 (2008). <https://doi.org/10.13182/FST08-A1654>
12. E. E. Salpeter. Electron Density Fluctuations in a Plasma, Physical Review, 120,1528 (1960).
13. H. Bindslev, On the Theory of Thomson Scattering and Reflectometry in a Relativistic Magnetized Plasma, Ph.D. thesis, Balliol College, Department of Engineering Science (1992).
14. Z.B. Shi et al., Calibration of a 32 channel electron cyclotron emission radiometer on the HL-2A tokamak, Rev. Sci. Instrum. 85, 023510 (2014).